ORIGINAL RESEARCH ARTICLE

Population Pharmacokinetic and Pharmacodynamic Analysis of GLPG1690, an Autotaxin Inhibitor, in Healthy Volunteers and Patients with Idiopathic Pulmonary Fibrosis

Amit Taneja[1] · Julie Desrivot[4] · Paul Matthias Diderichsen[3] · Roland Blanqué[1] · Lisa Allamasey[5] · Liesbeth Fagard[2] · Ann Fieuw[2] · Ellen Van der Aar[2] · Florence Namour[1]

Abstract

Background and Objectives GLPG1690 is an autotaxin inhibitor in development for the treatment of idiopathic pulmonary fibrosis. Several publications suggested a role of autotaxin in the control of disease-affected lung function and of lysophosphatidic acid in lung remodeling processes. The aim of the current article was to describe the exposure–response relationship of GLPG1690 and further develop a rational basis to support dose selection for clinical trials in patients with idiopathic pulmonary fibrosis.

Methods Two trials were conducted in healthy volunteers: in the first trial, GLPG1690 was administered as single doses from 20 mg up to 1500 mg, and subsequently in multiple daily doses of 300–1000 mg. In a second trial, the interaction of rifampin with 600 mg of GLPG1690 was evaluated. A third trial was conducted in patients with idiopathic pulmonary fibrosis administered 600 mg of GLPG1690 once daily for 12 weeks. The exposure–response (lysophosphatidic acid C18:2 reduction) relationship of GLPG1690 was first described using non-linear mixed-effects modeling and the model was subsequently deployed to simulate a lysophosphatidic acid C18:2 reduction as a biomarker of autotaxin inhibition in the dose range from 50 to 1000 mg once or twice daily.

Results The population pharmacokinetics and lysophosphatidic acid C18:2 response of GLPG1690 were adequately described by a combined population pharmacokinetic and pharmacokinetic/pharmacodynamic model. Dose, formulation, rifampin co-administration, health status (healthy volunteer vs. patient with idiopathic pulmonary fibrosis), and baseline lysophosphatidic acid C18:2 were identified as covariates in the model. The effect of dose on systemic clearance indicated that GLPG1690 followed a more than dose-proportional increase in exposure over the simulated dose range of 50–1000 mg once daily. Model-based simulations showed reductions in lysophosphatidic acid C18:2 of at least 80% with doses greater or equal to 200 mg once daily.

Conclusion Based on these results, 200 and 600 mg once-daily doses were selected for future clinical trials in patients with idiopathic pulmonary fibrosis.

✉ Amit Taneja
  Amit.Taneja@glpg.com

1 Galapagos SASU, 102 avenue Gaston Roussel, 93230 Romainville, France

2 Galapagos NV, Mechelen, Belgium

3 Certara Strategic Consulting, Breda, The Netherlands

4 Pierre Fabre, Toulouse, France

5 ALTEN Belgium, Brussels, Belgium

Key Points

Early clinical studies with GLPG1690, a potent and selective autotaxin inhibitor, showed a favorable pharmacokinetic/pharmacodynamic profile, demonstrating the ability to reduce plasma lysophosphatidic acid (LPA) C18:2 levels via inhibition of autotaxin.

A dose-dependent effect on LPA C18:2 levels was adequately described by a combined population pharmacokinetic/pharmacodynamic model.

Model-based simulations showed a plasma LPA C18:2 reduction of at least 80% with doses ≥ 200 mg. Simulations suggested that the putative therapeutic dose range for subsequent clinical trials in patients with idiopathic pulmonary fibrosis would lie between 200 and 600 mg once daily.

1 Background

Autotaxin (ATX) is an enzyme with lysophospholipase D activity, which is responsible for the production of lysophosphatidic acid (LPA), an important biological mediator of cell proliferation that underlies the development of pulmonary fibrosis [1]. Lysophosphatidic acid signals through multiple downstream receptors to control a range of cell activities such as migration, contraction, and survival; therefore, it plays important roles in bone development, [2] neurogenesis [3]. embryo implantation, [4], and the formation of blood and lymphatic vessels [5]. The most abundant LPA species in human plasma is LPA C18:2, with a fatty acid side chain of 18 carbon atoms including two unsaturated bonds. [6, 7]. Recently, a role for ATX and LPA in disease-affected lung function has been suggested. Increased levels of ATX and LPA seem to be associated with inflammatory and fibrotic conditions in the lung [1, 8, 9].

GLPG1690 (Fig. 1) is an orally available, potent selective inhibitor of ATX under development for the treatment of respiratory diseases such as idiopathic pulmonary fibrosis (IPF). In biochemical assays, the 50% inhibitory concentration value (IC_{50}) was 131 nM and 224 nM with human and mouse enzymes, respectively [10]. In vitro, the LPA production after human plasma incubation was inhibited by GLPG1690 with an IC_{50} of 242 nM. The IC_{50} difference was within two fold when the assay was performed in the absence of plasma, suggesting the low impact of plasma protein binding on the activity of the compound. The efficacy of GLPG1690 in a prophylactic bleomycin mouse model of lung fibrosis (measured as of lung weight and Ashcroft score) was reached with an exposure [area under the curve (AUC)] of 11 µg h/mL, corresponding to 26 µg h/mL in humans after inter-species correction for plasma protein binding, predicting an efficacious dose in humans of approximately 200 mg once daily (QD). In a mouse tobacco challenge model study, GLPG1690 significantly reduced the pulmonary infiltration of the total number of proinflammatory/profibrotic cells such as macrophages, neutrophils, and lymphocytes. The decrease was comparable to the positive control roflumilast. Plasma samples from a satellite group of animals in the same study showed a dose-dependent decrease in plasma LPA levels [11].

The pharmacokinetics and pharmacodynamics of GLPG1690 have been evaluated in a first-in-human (FiH) study in healthy volunteers (HVs) after single and multiple ascending doses (NCT02179502) [12] and in a proof-of-concept (PoC) study in patients with IPF (NCT02738801) [13, 14]. Additionally, a drug–drug interaction study was performed in HVs to determine the effect of repeated doses of rifampin [a strong and sensitive cytochrome P450 (CYP) 3A4 inducer as well as a P-glycoprotein (P-gp) inducer] on
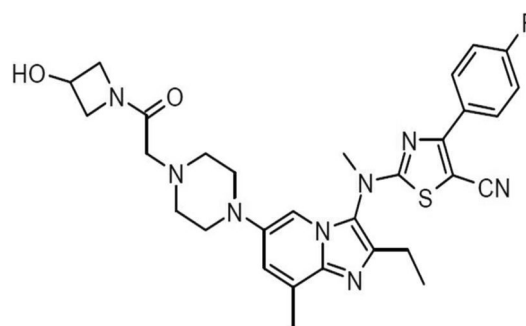

Fig. 1 Structure of GLPG1690

the pharmacokinetics of GLPG1690, which has been shown in vitro to be mainly metabolized via CYP3A4 (IND130687) as well as being a P-glycoprotein substrate (Fieuw et al., data on file). The aim of the current article was to describe the exposure–response relationship of GLPG1690 and further develop a rational basis to support dose selection for clinical trials in patients with IPF.

2 Methods

All studies were conducted in accordance with accepted standards for the protection of patient safety and welfare, and the principles of the Declaration of Helsinki and its amendments, and were in compliance with Good Clinical Practice. The FiH study protocol and informed consent were approved by the Ziekenhuis Netwerk Antwerpen Institutional Review Board (Belgium). The drug–drug interaction study protocol and informed consent were approved by the Midland Independent Review Board (USA). The PoC study protocol and informed consents were approved by the various local or central ethics review committees across 14 study sites that enrolled patients with IPF. All HVs and patients with IPF gave written informed consent prior to study initiation.

2.1 Trial Designs

A summary of the design features of all studies, including blood sampling for pharmacokinetics and pharmacodynamics is provided in Table 1.

2.1.1 First-in-Human Study (NCT02179502)

This was a randomized, double-blind, placebo-controlled, single-center study evaluating single and multiple ascending doses of GLPG1690 in healthy male volunteers (body mass index 20–30 kg/m^2, aged 18–50 years) [12]. Single doses of 20–1500 mg of GLPG1690 (oral suspension) and 300 mg of GLPG1690 (capsule) were taken by two cohorts

of eight volunteers each, who received treatment as ascending doses in an alternating fashion among the two cohorts. Subsequently, separate cohorts of eight volunteers (six taking GLPG1690 and two taking placebo) received twice-daily [BID] (150 mg) or once-daily (QD, 600 and 1000 mg) dosing for 14 days. All doses were administered after a standard breakfast or evening meal (approximately 533 kcal).

2.1.2 Drug–Drug Interaction Study (IND130687)

This was an open-label, single-center, drug–drug interaction study evaluating the effect of repeated doses of rifampin (600-mg capsule) for 10 days on the single-dose pharmacokinetics of GLPG1690 (600-mg capsule) in 18 healthy male volunteers (body mass index 20–30 kg/m^2, aged 18–50 years) (Fieuw et al., data on file). Blood samples were collected for pharmacokinetic (PK) assessment before and after repeated dosing with rifampin.

2.1.3 Proof-of-Concept Study in Patients with Idiopathic Pulmonary Fibrosis (NCT02738801)

The exposures of GLPG1690 and LPA C18:2 biomarker responses were evaluated in 23 patients with a confirmed IPF diagnosis who received GLPG1690 600 mg QD (capsule) or placebo for 12 weeks ($n=6$ placebo and 17 active) [13]. Included patients were not allowed to take experimental or approved IPF therapies (such as pirfenidone and nintedanib) within 4 weeks before the screening period.

2.2 Bioanalytical, Pharmacokinetic, and Pharmacodynamic Assessments

Blood samples for PK and pharmacodynamic (PD) assessments were collected in tubes containing lithium heparin as an anticoagulant to obtain plasma for the determination of GLPG1690 and of LPA C18:2. Within 30 min after blood collection, the plasma was separated in a refrigerated centrifuge (4–8 °C) for 10 min at approximately 1500 g and stored at − 20 °C until analysis.

Plasma concentrations of GLPG1690 were determined using a validated liquid-chromatography tandem mass spectrometry assay. To each 20-µL plasma sample, 900 µL of 0.06 M hydrochloric acid, 50 µL of methanol, and 50 µL of the internal standard (40 ng/mL of deuterated GLPG1690) were added. Samples were mixed and the supernatant loaded onto a solid-phase extraction plate. After washing (1 mL of 0.06 M hydrochloric acid followed by 1 mL Elix and 1 mL of methanol), the samples were eluted (1 mL NH$_4$OH 1% in acetone) and then evaporated to dryness at 50 °C under nitrogen. The extraction yield of GLPG1690 under these conditions was constant over

the concentration range tested (3.00–800 ng/mL), ranging from 104% to 121%. The reconstituted samples (300 µM of acetonitrile in water 25:100 v/v + 0.01% NH$_4$OH) were injected into an AB SCIEX API 4000 liquid-chromatography tandem mass spectrometry equipped with an Xbridge C18 column. GLPG1690 was detected in positive mode using multiple-reaction monitoring. Typical retention time was 3.2 min. Quantification was performed using peak area ratios and standard curves (with $y = a + bx$, weighting factor $= 1/x^2$) prepared from calibration standards. The lower limit of quantification was 1.00 ng/mL. The between- and within-run precision for quality controls expressed as a coefficient of variation were not greater than 16.9%, with deviations from nominal concentrations of no more than 6.3%.

Plasma concentrations of LPA C18:2 were measured using a validated liquid-chromatography tandem mass spectrometry method. This method was not quantitative because of the presence of endogenous LPA levels in plasma. The method was based on quantifying the ratio of LPA C18:2/internal standard (LPA C17:0) peak area. This value was used to determine the percentage of reductions in LPA by comparing LPA C18:2/IS in a sample collected at each time point with the one in the baseline sample. The quality-control samples were prepared and used to qualify each analytical batch at final concentrations of 0 (no LPA spike), 45, and 182 nM. Precision was estimated for each run using $\pm 15\%$ as the acceptance criterion (at least 67% and at least one quality control per concentration had to be within 15% precision). The effect of GLPG1690 on LPA C18:2 values was expressed as the percentage reduction vs. baseline: % LPA C18:2 peak area ratio reduction from baseline $= 100 - (100 \times$ visit/baseline).

2.3 Population Pharmacokinetic and Pharmacokinetic/Pharmacodynamic Modeling

The population analyses and statistical methods were based on the US Food and Drug Administration [15] and European Medicines Agency guidance documents [16].

2.3.1 Population Pharmacokinetic and Pharmacokinetic/Pharmacodynamic Data Assembly

Dose records describing GLPG1690 dosing amounts and actual time of administration, baseline covariates, and measured GLPG1690 plasma concentrations were merged and formatted as a NONMEM-compatible analysis dataset using SAS® (Version 9.4, SAS Institute, Cary, NC, USA). All data assembly programs were documented and archived to maintain an audit trail. Plasma LPA C18:2 reported for individual subjects treated with GLPG1690 was included in

Table 1 Summary of included trials and respective design features

Study	Study objectives	Subject (age, y)	Main inclusion criteria/concomitant medications	Study design	Formulation/dosing	Sampling design
Phase I (FiH), NCT02179502	Safety, tolerability, PK, and PD of single and multiple ascending oral doses of GLPG1690	Part 1: 16 male volunteers (18–50)	Good health with no clinically significant deviation from normal in terms of medical history, physical examinations, ECGs, or clinical laboratory parameters. No co-medications except acetaminophen allowed	Randomized, double-blind, placebo-controlled	Single doses: 20–1500 mg (oral suspension) and 300 mg (capsule) Fed state	PK/PD: before dose and at 0.5, 1, 2, 4, 6, 8, 12, 24 and 48 h post-dose
		Part 2: 24 male volunteers (18–50)			Multiple doses: 150 mg BID, 600 and 1000 mg QD for 14 d (oral suspension) Fed state	PK/PD: days 1 and 14, before dose and at 0.5, 1, 2, 4, 6, 8, 12, 24, and 48 h post-dose. Additional PK samples pre-dose on days 3, 4, 5, 6, 8 and 15
Phase I (DDI), IND 130687	DDI with rifampin	18 male volunteers (18–50)	Good health with no clinically significant deviation from normal in terms of medical history, physical examinations, ECGs, or clinical laboratory parameters. No concomitant medications except acetaminophen	Non-randomized, open-label	Single doses: 600 mg (capsule) taken before and after 10 d of rifampin 600 mg QD (capsule) Fed state	PK: on days 1 and 12, before and at 1, 2, 3, 4, 5, 6, 7, 8, 10, 12, and 24 h post-dose
Proof-of-concept, NCT02738801	Safety, tolerability, PK, and PD and exploratory efficacy	23 male or female patients with IPF (52–79)	Confirmed diagnosis of IPF, a forced vital capacity of ≥50% predicted of normal, carbon monoxide lung diffusion capacity ≥30% predicted of normal, forced expiratory volume in 1 s ≥ 0.70	Multicenter, randomized, double-blind, parallel-group, placebo-controlled, exploratory	600 mg QD (capsule) for 12 wk (i.e., 84 d)	PK: pre-dose samples on days 7, 14, 28, 56, and 84. Additional PK samples at 1.5, 4, and 6 h post-dose on day 28 PD: pre-dose samples on days 28 and 84, and 1.5 and 6 h post-dose on day 28. A follow-up sample was collected on day 98
Proof of concept, NCT02738801	Safety, tolerability, PK, and PD and exploratory efficacy	23 male or female patients with IPF (52–79)	Confirmed diagnosis of IPF, a forced vital capacity of ≥50% predicted of normal, carbon monoxide lung diffusion capacity ≥30% predicted of normal, forced expiratory volume in 1 s ≥ 0.70	Multicenter, randomized, double-blind, parallel-group, placebo-controlled, exploratory	600 mg QD (capsule) for 12 wk (i.e., 84 d)	PK: pre-dose samples on days 7, 14, 28, 56, and 84. Additional PK samples at 1.5, 4, and 6 h post-dose on day 28 PD: pre-dose samples on days 28 and 84, and 1.5 and 6 h post-dose on day 28. A follow-up sample was collected on day 98

BID twice daily, *DDI* drug–drug interaction, *ECG* electrocardiogram, *FiH* first-in-human, *IND* Investigational New Drug, *IPF* idiopathic pulmonary fibrosis, *PD* pharmacodynamics, *PK* pharmacokinetics, *QD* once daily

the analysis dataset for simultaneous fitting of PK parameters and the PK/PD relationship.

2.3.2 Exploratory Data Analysis

GLPG1690 plasma concentrations and plasma LPA C18:2 vs. time profiles were explored graphically for the identification of potential outliers. The graphical analysis of GLPG1690 plasma concentrations and plasma LPA C18:2 provided initial directions to the structural, statistical, and residual error model components of the combined population pharmacokinetic and PK/PD model. Covariate summary statistics were provided across studies.

2.3.3 Covariates

Covariate analysis was conducted as part of the population PK and PK/PD analyses to explain variability in GLPG1690 plasma concentrations and observed LPA C18:2 responses, respectively. The covariate-tested models were demographics (PK and PK/PD models), formulation, and rifampin administration (PK model only), baseline LPA, single vs. multiple ascending dose parts of the FiH study, and HV vs. IPF patient status (PK/PD model only).

2.3.4 Starting Population Pharmacokinetic Model

The time course of GLPG1690 plasma concentrations was described by a two-compartment structural model with oral absorption and linear elimination. Different random-effect models, and the effect of extrinsic covariates (e.g., rifampin administration, formulation) on different model parameters were evaluated on the starting model resulting in the base model.

2.3.5 Pharmacokinetic and Pharmacokinetic/ Pharmacodynamic Full and Final Model Development

The association between subject-level covariates, PK parameters, and predictors of plasma LPA C18:2 was evaluated in a stepwise manner, applying an iterative addition and deletion covariate selection strategy. Model selection was performed based on the likelihood ratio test and the NONMEM objective function value (OFV) by iteratively adding the most significant of the evaluated covariate-parameter relationships until no more statistically significant covariates (at $p = 0.01$) were found. Subsequently, the least significant covariate was eliminated

in a backward deletion procedure until no non-significant covariates (at $p = 0.001$) were left in the model. Finally, covariates that did not lead to at least a 10% reduction in the corresponding between-patient random-effect variance (ω^2) were excluded from the covariate model. The PK/PD stepwise covariate model building was automated by the stepwise covariate modeling script included in the PsN toolkit.

2.3.6 Pharmacokinetic Model Evaluation

Alternative models were compared based on the model fit (i.e., OFV), precision of parameter estimates (relative standard error, %RSE), condition number, and random-effect and residual error model variances. The model with a statistically significantly lower objective function was preferred. However, it could have been discarded based on the estimated uncertainty of any fixed model parameters, if any parameter estimate appeared implausible, or if diagnostic plots and methods (e.g., bootstrap evaluation, visual predictive check) indicated that the model showed substantial bias or was unable to describe the trends and variability of the observed data.

2.3.7 Pharmacokinetic/Pharmacodynamic Modeling of Plasma Lysophosphatidic Acid C18:2

A PK/PD analysis was conducted to describe the relationship between GLPG1690 and LPA C18:2 plasma concentrations. The PK/PD analysis reported individual plasma LPA C18:2 (from the FiH and PoC studies) to individual-predicted exposures in a regression analysis framework. The HVs participating on multiple occasions in the SAD part of the FiH study were considered as independent volunteers in the analysis, given the washout period (1 week) between occasions. This approach implicitly accounted for between-occasion variability. The starting model was a direct response (regression) model under the assumption that the delay between changes in GLPG1690 and LPA C18:2 plasma concentrations was negligible.

Model variations including different random-effect models, and structural covariates (e.g., study subpopulations) on different model parameters, non-linearities (Hill factors), and the impact of delays between PK and PD responses were compared to the starting model. The statistical model was built using the same principles as used for the population PK analysis and the developed PK/PD model was evaluated using similar diagnostic methods. Outlying data records with an unreasonably large time

period since the last dose or large conditional weighted residuals based on a preliminary model were flagged for exclusion from the analysis.

2.3.8 Model Diagnostics and Evaluation

Alternative models were compared based on the model fit (i.e., OFV), precision of parameter estimates (%RSE), condition number, and random-effect and residual error model variances. Diagnostics included comparative objective function values, plausibility of parameter estimates, and goodness-of-fit plots.

A non-parametric bootstrap was performed to rule out substantial bias in the estimates. Additionally, visual predictive checks were performed, where 1000 replicates of the analysis dataset were performed and the quartiles of observed data were superposed on the simulated data to demonstrate the ability of the model to adequately describe the mean trend and variability in the observed data.

2.3.9 Model-Based Simulations

Typical Patient Simulations The developed combined population PK and PK/PD model was simulated to elucidate the relationship between dose, exposure, and plasma LPA C18:2 in the typical patient with IPF, incorporating uncertainty in the model parameter estimates. Two hundred and fifty sets of parameters from the variance–covariance matrix of the estimates were sampled. Patient covariates identified in the population PK and PK/PD analyses were set to typical (i.e., median or most frequent) values, while random effects (random effects are denoted as ETA in NONMEM) were set to zero. The default simulation scenario was a typical patient with IPF treated with a GLPG1690 capsule, not taking rifampin, with a baseline plasma LPA C18:2 of 0.36. Health status was not found to be a covariate on any of the PD parameters; hence, the maximal (possible) plasma LPA C18:2 reduction (I_{max}) was based on the value estimated for the pooled HV and patient data.

The simulated steady-state exposure was summarized as maximal GLPG1690 plasma concentration (C_{max}) and exposure during a 24-h interval (AUC_{24h}) with a 95% confidence interval (CI) for total daily doses of 50, 100, 200, 300, 600, and 1000 mg administered QD or BID. Similarly, simulated plasma LPA C18:2 was summarized as the maximal plasma LPA C18:2 reduction from baseline and area under the (baseline-corrected) plasma LPA C18:2 effect curve during a 24-h interval ($AUEC_{24h}$) with a 95% CI for the same set of GLPG1690 doses.

Individual Subject Simulations Simulations accounting for between-subject variability were performed to describe the distribution of PK and PD responses predicted for total QD doses between 50 and 1000 mg. The baseline plasma LPA C18:2 (LPA C18:2$_{BL}$) was sampled from a uniform distribution covering the range of reported values for 15 patients in the PoC patient study (0.14–0.59), excluding one patient with a reported LPA C18:2$_{BL}$ value of 1.3, which was considered an outlier. Unexplained between-patient variability was accounted for by sampling random effects from the variance–covariance matrix describing patient-level random effects in the final model. The simulations included 10,000 virtual patients replicated across seven GLPG1690 dose levels from 50- to 1000-mg QD dosing.

The individual patient simulations results were summarized as the 2.5th, 10th, 25th, and 50th (median) percentile of individual C_{max}, AUC_{24h}, maximal plasma LPA C18:2 reduction (I_{max}), and LPA C18:2 $AUEC_{24h}$ with 90% prediction intervals. Parameter uncertainty was not accounted for in the individual patient simulations, reflecting an assumption that the maximum likelihood parameters estimated by the model were close to the true values.

3 Results

3.1 Subject/Patient Disposition and Dataset Summary

A summary of the number of subjects and GLPG1690 and LPA C18:2 plasma concentrations included in the analysis dataset, as well as subject covariates and the number of PK/PD samples according to the GLPG1690 regimen included in the analysis dataset are summarized in Table 2. The concentrations below the limit of quantification (1.00 ng/mL) excluded from the dataset represented 11% (166/1514) of the total number of values of the dataset.

To illustrate the PK data used in the PK/PD modeling, a scatterplot of the dose–normalized GLPG1690 plasma concentrations as a function of time since the last dose is presented in Fig. 2. Additionally, selected LPA C18:2 vs. time profiles for single doses ranging from 20 to 1500 mg and repeat doses of 150, 600, and 1000 mg, each given QD or BID (150 mg) for 14 days, are also presented.

Table 2 Subject demographics, baseline characteristics, and number of samples used/excluded in the population pharmacokinetic/pharmacodynamic analysis

| Demographic, mean (range) or %	First-in-human study, SAD (NCT02179502)	First-in-human study, MAD (NCT02179502)	Drug–drug interaction study (IND130687)	PoC study (NCT02738801)
Number of subjects in the study	16	24	18	23
Sex	100% male	100% male	100% male	56.25% male, 43.75% female
Age, y	39.5 (21–49)	39.2 (24–49)	34.9 (21–49)	66.8 (54–79)
Weight, kg	80.1 (69.40–98.8)	80.30 (64.20–98)	83.80 (66.75–104.50)	83.10 (66.30–110)
BMI, kg/m^2	24.5 (20.0–30.0)	25.4 (22.0–30.0)	26.1 (20.6–29.4)	29.7 (24.8–39.1)
LPA C18:2$_{BL}$	0.474 (0.239–0.884)	0.174 (0.104–0.319)	N/A	0.329 (0.136–1.305)
Number of NONMEM ID/ number of PK samples	48/417	18/414	18/393	16/122
Number of NONMEM ID/ number of PD samples	42/477	48/342	N/A	16/75
Number of PK samples excluded	–		1 sample was missing sample time 1 sample with concentration < LOQ at 72 h since last dose	15 duplicate pre-dose concentrations were excluded 3 samples were missing values 1 sample with concentration < LOQ at 95.5 h since last dose
Number of PD samples excluded	1 sample was missing a LPA value		–	1 sample collected approximately 9 wk since last dose

Median (range) presented for demographic variables

BMI body mass index, *IND* Investigational New Drug, *LOQ* limit of quantitation, *LPA* lysophosphatidic acid, *LPA$_{BL}$* baseline lysophosphatidic acid, *MAD* multiple ascending dose, *N/A* not applicable, *PD* pharmacodynamics, *PK* pharmacokinetics, *PoC* proof-of-concept, *SAD* single ascending dose
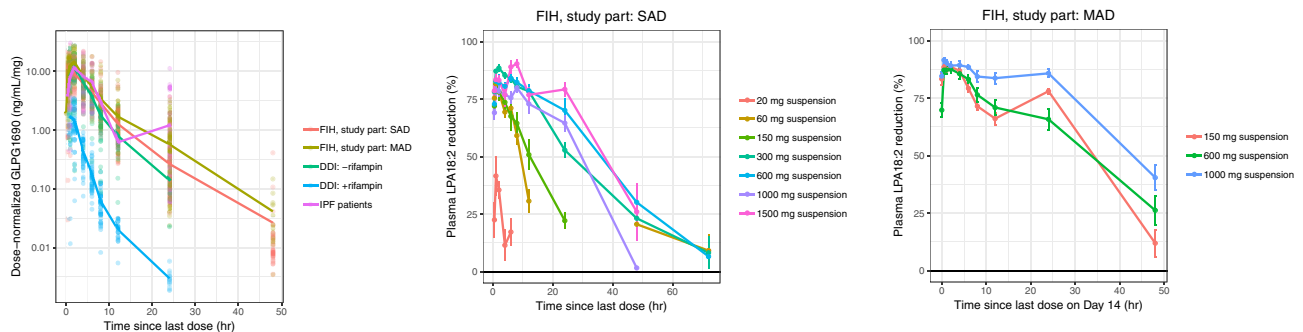
Fig. 2 Dose-normalized GLPG1690 concentration–time and lysophosphatidic acid (LPA) C18:2–time plots of data used for the population pharmacokinetic and pharmacodynamic analyses. *DDI* drug–drug interaction, *FiH* first-in-human, *IPF* idiopathic pulmonary fibrosis, *MAD* multiple ascending dose, *SAD* single ascending dose
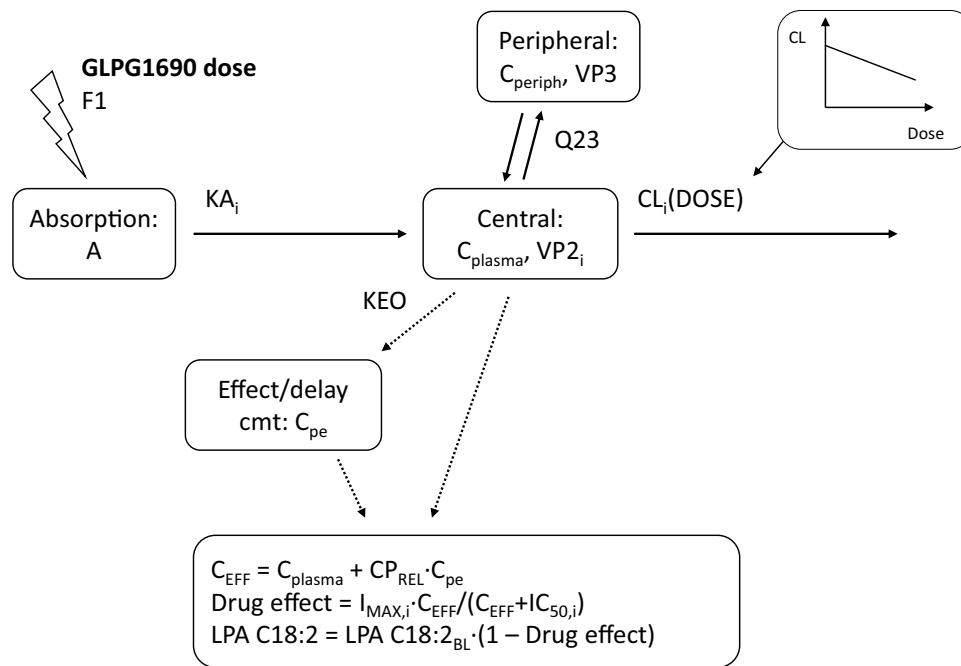
Fig. 3 Structure of the combined GLPG1690 population pharmacokinetic and plasma lysophosphatidic acid (LPA) C18:2 pharmacokinetic/pharmacodynamic model. *A* GLPG1690 amount in the absorption compartment, C_{EFF} effective concentration (weighted sum of plasma and effect compartment concentration), CL_{SLP} slope of the linear relationship between GLPG1690 dose and apparent clearance, C_{plasma} *and* C_{periph} GLPG1690 concentration in the central (plasma) and peripheral compartments, CP_{REL} weighting factor between plasma and effect compartment concentration, C_{pe} (hypothetical)

effect compartment concentration, *F1* bioavailability, $I_{max,i}$ maximal reduction in plasma LPA C18:2, KA_i absorption rate constant, *KEO* rate constant of the effect compartment, Q_{23} apparent inter-compartmental clearance, $TVCL_i$ typical apparent clearance for subject *i*, *VP2* apparent volume of distribution of central compartment, *VP3* apparent volume of distribution of peripheral compartment. For simplicity, covariate relations (apart from dose effect on clearance) and definition of random effects are not explicitly shown

3.2 GLPG1690 Population Pharmacokinetic/Pharmacodynamic Model

The observed concentration and LPA C18:2 response was described in a combined population PK and PK/PD model, as shown in Fig. 3.

$$\frac{d}{dt}A = -KA_i \cdot A$$

$$VP2 \cdot \frac{d}{dt}C_{plasma} = KA_i \cdot A - Q23 \cdot \left(C_{plasma} - C_{periph}\right) - CL_i(DOSE) \cdot C_{plasma}$$

$$VP3 \cdot \frac{d}{dt}C_{periph} = Q23 \cdot \left(C_{plasma} - C_{periph}\right)$$

$$\frac{d}{dt}C_{pe} = KEO \cdot \left(C_{plasma} - C_{pe}\right)$$

$$CL_i(DOSE) = TVCL_i \cdot \left(1 - CL_{SLP} \cdot DOSE\right)$$

$$C_{EFF} = C_{plasma} + CP_{REL} \cdot C_{pe}$$

$$LPA\ C_{18:2} = LPA\ C_{18:2,BL} \cdot \left(1 - \frac{I_{MAX,i} \cdot C_{EFF}}{C_{EFF} + IC_{50,i}}\right)$$

The pharmacokinetics of GLPG1690 was described by a two-compartment model with first-order absorption and dose-dependent elimination, where the apparent systemic clearance (CL) decreased with increasing doses. This is further depicted in Fig. 3, and the transfer of mass

balance is described with the help of differential equations. To elaborate further, GLPG1690 is absorbed into the central compartment following oral dosing. There is exchange of drug between the central and a peripheral compartment, governed by a first-order process, whereby Q_{23} is the inter-compartmental clearance. It undergoes elimination from the central compartment in a dose-dependent manner, i.e., the higher the dose, the lower the clearance.

Visual exploration of the PK and PD data revealed a transient hysteresis and this was described with a hypothetical effect compartment (C_{pe}), see Figs. S1 and S2 of the Electronic Supplementary Material (ESM). The observed plasma LPA C18:2 could be described by an I_{max} function driven by "effective concentration", defined as a weighted sum of plasma GLPG1690 and "effect site" concentration in the said hypothetical effect compartment. Inclusion of the effect compartment resulted in a statistically significant improvement of the model (46 points reduction of OFV for 2 *df*, $p < 0.0001$). The estimated weighting factor allowed the model to describe a biphasic plasma LPA C18:2 response to GLPG1690 plasma concentrations composed of an immediate component driven by plasma the GLPG1690

Table 3 Final model parameter estimates and bootstrap results

Parameter	Estimate in physical units	Estimate (%RSE)	BSV variance (%RSE)	Bootstrap 95% CI of estimate	Bootstrap 95% CI estimate of BSV
CL[a]	23.3 L/h (54.2%cv)	3.15 (2.22)	0.294 (13)	2.998–3.269	0.1543–0.4553
VP2[a]	14.1 L (93.7%cv)	2.65 (4.48)	0.877 (14)	2.445–2.888	0.381–1.449
CL × VP2 covariance	70.3% (correlation)	–	0.357 (18)	–	0.135–0.6288
KA[a]	0.222/h (13.9%cv)	−1.51 (3.28)	0.0194 (27.7)	− 1.591 to − 1.389	0.00294–0.04116
Q_{23}[a]	1.14 L/h	0.130 (153)	–	−0.2298 to 0.5158	–
VP3[a]	12.5 L	2.53 (5.01)	–	2.312–2.778	–
KA (capsule)	16.2% change	0.162 (42.1)	–	0.04168–0.285	–
Relative bioavailability F1 with DDI[a]	9.94%	− 2.31 (5.84)	–	− 2.58 to − 2.057	–
KA with DDI	117% change	1.17 (13.2%)	–	0.8704–1.54	–
CL(DOSE)	−0.0415% change/mg	0.000415 (12.5)	–	0.0003045–0.0004993	–
I_{max}[b]	90.8%	1.33 (4.15)	0.0324 (10.8)	1.218–1.499	0.0161–0.044
IC_{50}[a]	114 ng/mL (35.9%cv)	4.74 (3.08)	0.129 (15.8)	4.461–5.095	0.04571–0.2102
KEO[a]	0.0982/h	− 2.32 (5)	–	− 2.562 to − 2.11	–
CP_{REL}[a]	0.303	− 1.20 (16.2)	–	− 1.616 to − 0.745	–
I_{max} at occasion 2 of the FIH study, SAD part	83.33%	− 0.36 (19.9)		− 0.5861 to − 0.2118	
I_{max} at occasion 3 of the FIH study, SAD part	80.97%	−0.4504 (18.4)		−0.6433 to −0.2277	
I_{max} at day 14 and later of the FIH study, MAD part	93.72%	0.2043 (13.9)		0.1385–0.2611	
GLPG1690 RUV in patients with IPF[a]	23.3% change	0.209 (50.5)	–	−0.03705 to 0.4562	–
Plasma LPA C18:2 RUV in patients with IPF[a]	64.9% change	0.500 (22.6)	–	0.2115–0.721	–
IC_{50} (LPA C18:2$_{BL}$)[c]	−4.41% change/+ 10%	−0.473 (23.8)	–	− 0.7344 to − 0.1537	–
I_{max} (LPA C18:2$_{BL}$)[d]	91.7% at typical baseline +0.1	0.5805 (26)	–	0.2506–1.389	–
VP2 in IPF patients	559% change	5.59 (24.2)	–	2.671–8.647	–
GLPG1690 RUV	44.8%cv	0.200 (5.86)	–	0.1514–0.2398	–
Plasma LPA C18:2 RUV	27.6%cv	0.0762 (3.09)	–	0.06678– 0.08577	–

CI confidence interval, *CL* clearance, *CP_{REL}* weighting factor between plasma and effect compartment concentration, *DDI* drug–drug interaction, *FIH* first-in-human, *F1* bioavailability, *IC_{50}* 50% inhibitory concentration value, *I_{max}* maximal reduction of plasma LPA C18:2, *IPF* idiopathic pulmonary fibrosis, *KA* absorption rate constant, *KEO* rate constant of the effect compartment, *LPA* lysophosphatidic acid, *LPA C18:2* baseline lysophosphatidic acid, *MAD* multiple ascending dose, *Q_{23}* apparent inter-compartmental clearance, *RUV* residual unexplained variability, *SAD* single ascending dose, *VP2* apparent volume of distribution of central compartment, *VP3* apparent volume of distribution of peripheral compartment

[a]Log-transformed parameter

[b]Probit transformed parameter

[c]Power function covariate relation (as a function of baseline LPA C18:2) on log-transformed parameter

[d]Linear covariate relation (as a function of baseline LPA C18:2) on probit-transformed parameter

concentration and a delayed component driven by the effect-site concentration.

Correlated random effects were included on CL and the apparent volume of distribution of central compartment (VP2). In addition, random effects on GLPG1690 absorption rate, and the I_{max} and IC_{50} parameters describing the PK/PD relationship were included. Including a covariance term on I_{max} and IC_{50} did not improve the model. The model described the log-transformed GLPG1690 plasma concentration and plasma LPA C18:2 with residual unexplained variability described by an additive residual error model. A study effect was included on the residual unexplained variability variance, allowing the model to describe a higher variance in the PoC patient study.
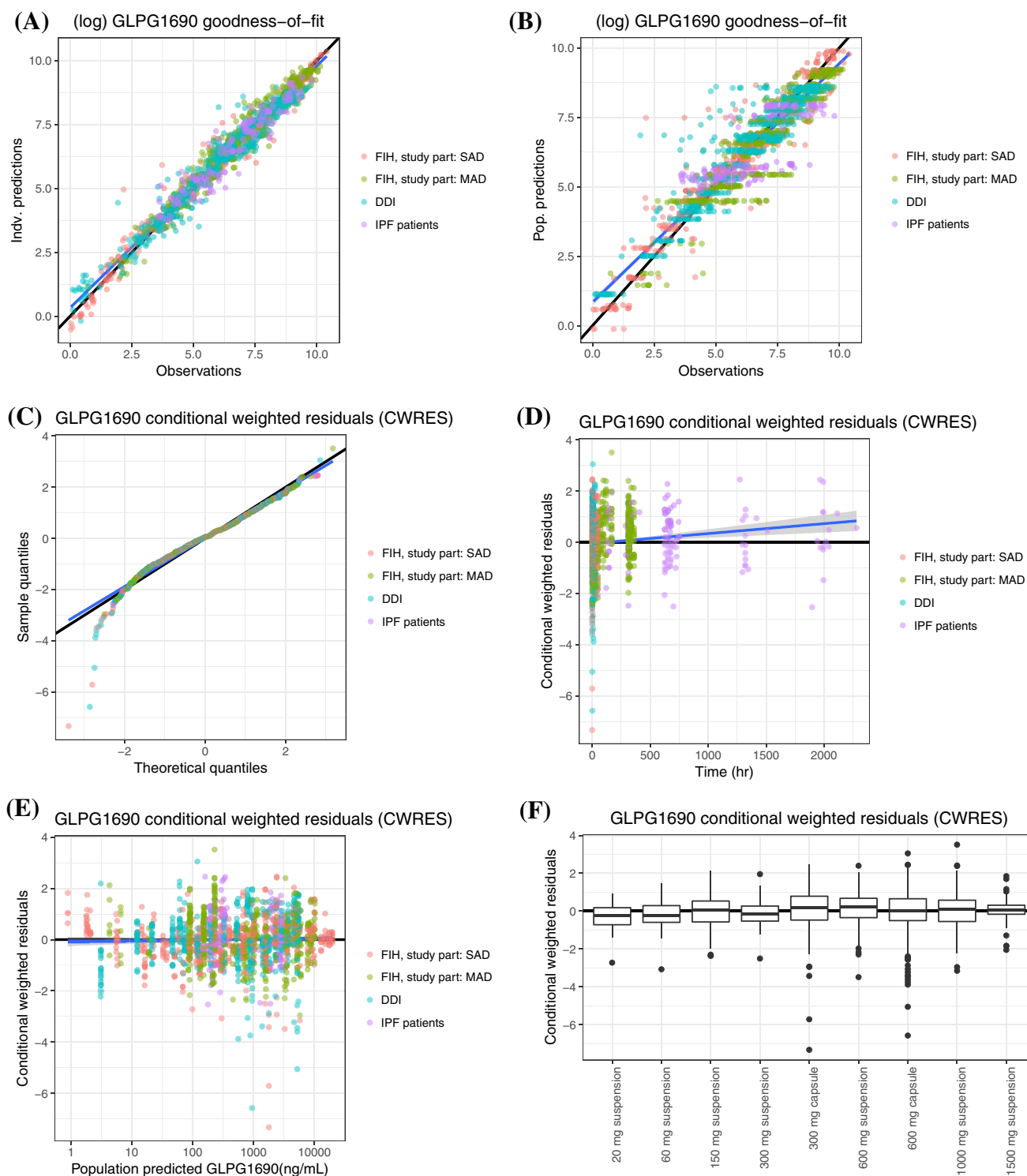
Fig. 4 Goodness-of-fit assessment comparing observed GLPG1690 plasma concentrations with the corresponding individual (**a**) and population predictions (**b**), Q–Q plot of conditional weighted residuals (**c**), and conditional weighted residuals vs. time, population-predicted GLPG1690 plasma concentration, and by treatment group (**d**–**f**). The *solid black* and *blue lines* show the line of unity and linear regression (with 95% confidence interval), respectively. *DDI* drug–drug interaction, *FiH* first-in-human, *IPF* idiopathic pulmonary fibrosis, *MAD* multiple ascending dose, *SAD* single ascending dose
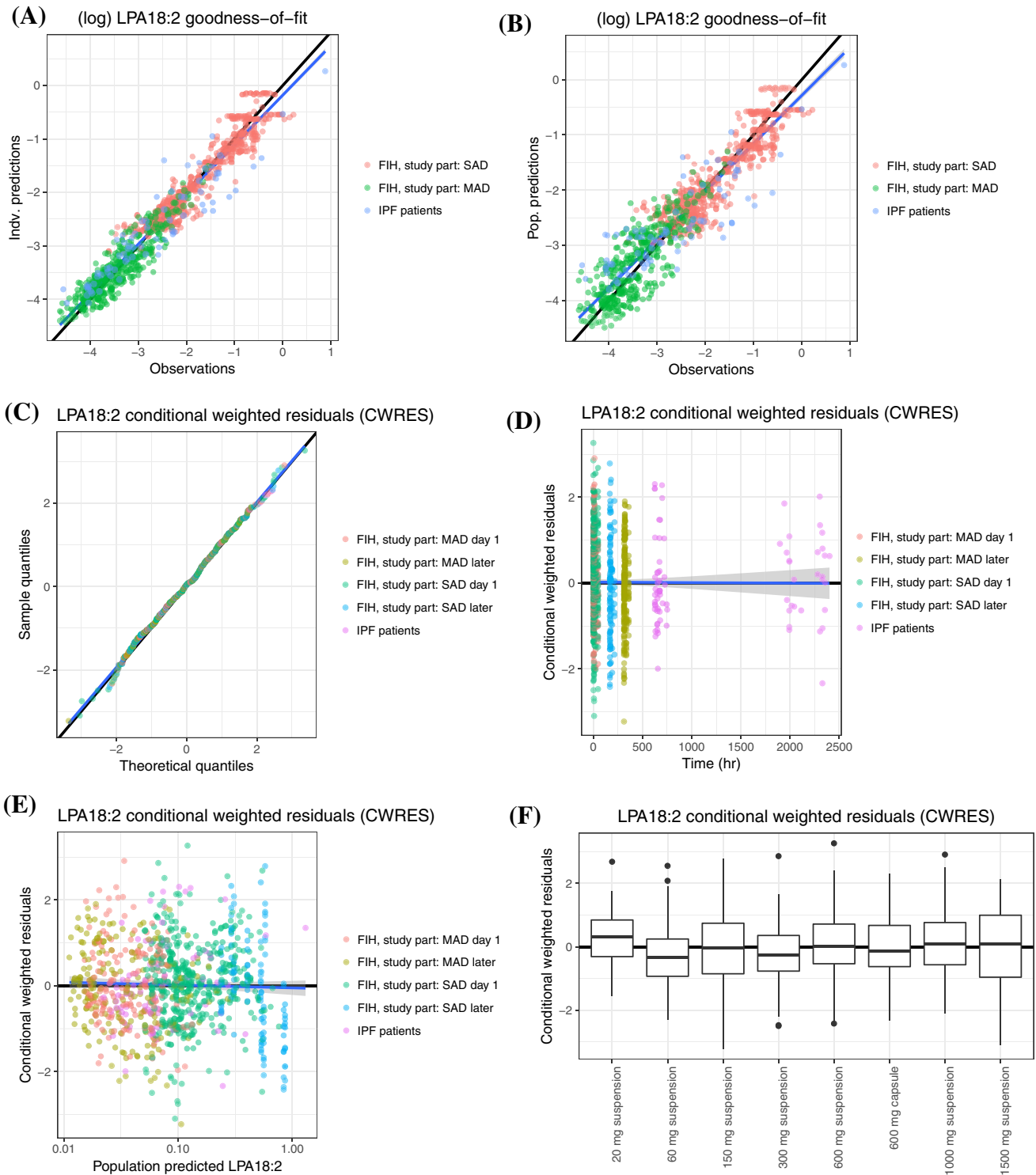
Fig. 5 Goodness-of-fit assessment comparing observed plasma lysophosphatidic acid (LPA) C18:2 with the corresponding individual (**a**) and population predictions (**b**) and Q–Q plot of conditional weighted residuals [CWRES] (C), and CWRES vs. time, population-predicted LPA C18:2, and by treatment group (**d**–**f**). The *solid black* and *blue lines* show the line of unity and linear regression (with 95% confidence interval), respectively. *DDI* drug–drug interaction, *FiH* first-in-human, *IPF* idiopathic pulmonary fibrosis, *MAD* multiple ascending dose, *SAD* single ascending dose
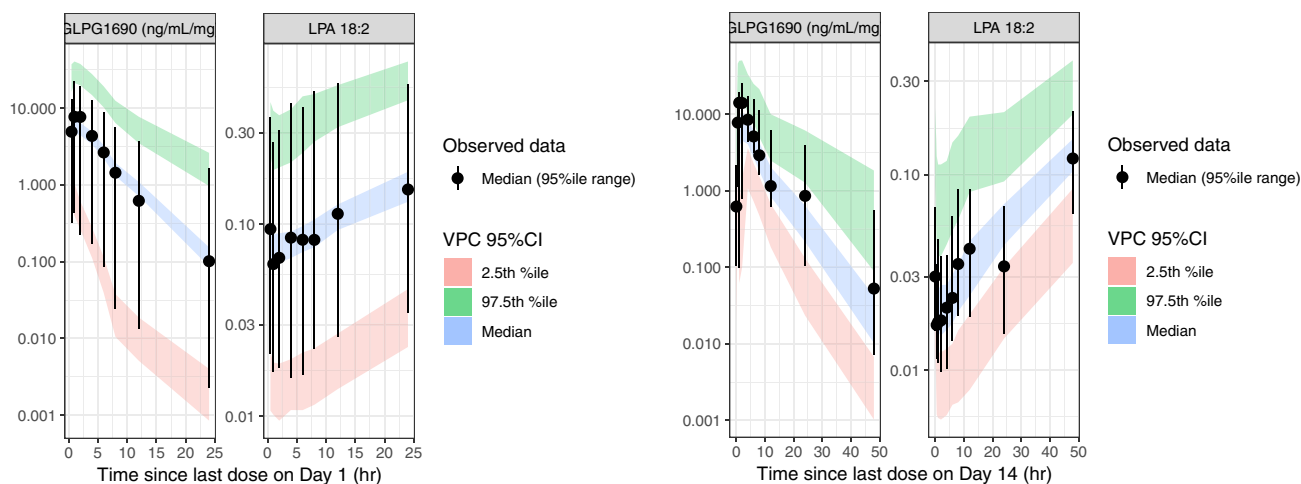
Fig. 6 Visual predictive checks (VPC) of all data on day 1 (*left*) and day 14 (*right*). *LPA* lysophosphatidic acid. *CI* confidence interval

A summary of estimated parameter values of the final GLPG1690 population PK and plasma LPA C18:2 PK/PD model is shown in Table 3. Most parameters were estimated with residual standard errors (RSEs) well below 50%. An exception was the apparent inter-compartmental clearance (Q_{23}). However, because this was modeled as a log-transformed parameter, this was considered acceptable. Additionally, the relative increase in the RUV of the GLPG1690 plasma concentration in the patient study was estimated with a RSE slightly above 50%. However, for symmetry reasons (e.g., the similar effect estimated on plasma LPA

C18:2 RUV), the parameter was retained in the model. The maximum likelihood estimate and the appropriateness of the parametric confidence intervals were confirmed by a bootstrap evaluation of the model. Two and eight runs out of 250 were discarded because of non-convergence and parameter estimates near a boundary, respectively.

3.3 Covariate Effects

Subject health status (HV vs. IPF) was included as a covariate on the VP2 with ~560% increased volume in patients

Table 4 Simulated typical patient dose–response relationship of GLPG1690 pharmacokinetics and plasma lysophosphatidic acid (LPA) C18:2 pharmacodynamics at steady state

GLPG1690 treatment (mg total daily dose)	GLPG1690 C_{max} (ng/mL) [95% CI]	GLPG1690 AUC (μg/mL h) [95% CI]	Maximal plasma LPA C18:2 reduction (%) [95% CI]	Plasma LPA C18:2 AUEC (%h) [95% CI]
50 QD	204 [172–254]	2.19 [1.96–2.58]	60.7 [55.2–66.6]	1010 [902–1140]
50 BID	124 [108–147]	2.19 [1.96–2.58]	51.8 [46.8–57.8]	1100 [970–1240]
100 QD	413 [348–514]	4.48 [4.02–5.25]	73 [68.9–76.9]	1360 [1240–1480]
100 BID	252 [220–299]	4.48 [4.02–5.25]	66.3 [62–70.6]	1470 [1360–1580]
150 QD	626 [528–780]	6.86 [6.17–8.02]	78.2 [75.1–81]	1550 [1440–1660]
150 BID	385 [336–457]	6.86 [6.17–8.02]	73.1 [69.5–76.5]	1650 [1570–1750]
200 QD	845 [713–1050]	9.36 [8.43–10.9]	81.1 [78.7–83.3]	1670 [1570–1770]
200 BID	522 [456–620]	9.36 [8.43–10.9]	77 [74.1–79.8]	1770 [1690–1840]
300 QD	1300 [1100–1610]	14.7 [13.3–16.9]	84.3 [82.4–86]	1820 [1740–1890]
300 BID	811 [711–962]	14.7 [13.3–16.9]	81.4 [79.3–83.4]	1900 [1840–1950]
600 QD	2830 [2370–3480]	34.3 [31.1–38.5]	87.7 [86.3–89.2]	2020 [1950–2050]
600 BID	1830 [1610–2150]	34.3 [31.1–38.5]	86.4 [84.9–87.9]	2050 [2010–2090]
1000 QD	5420 [4460–6690]	73.3 [63.4–84.2]	89.2 [87.6–90.8]	2110 [2050–2140]
1000 BID	3720 [3150–4390]	73.3 [63.4–84.2]	88.6 [87–90.2]	2120 [2080–2160]

AUC area under the curve, *AUEC* area under the effect curve, *BID* twice daily, *CI* confidence interval, *C_{max}* maximum plasma concentration, *QD* once daily

Fig. 7 Percentiles of individual-simulated steady-state area under the curve (AUC, top-left), maximum plasma concentration (C_{max}, top-right), area under the effect curve (AUEC, bottom-left), and maximal plasma lysophosphatidic acid (LPA) C18:2 reduction (bottom-right) at GLPG1690 doses between 50 and 1000 mg once daily
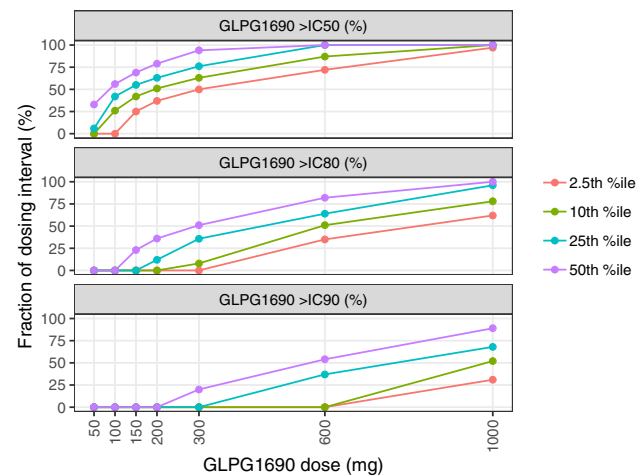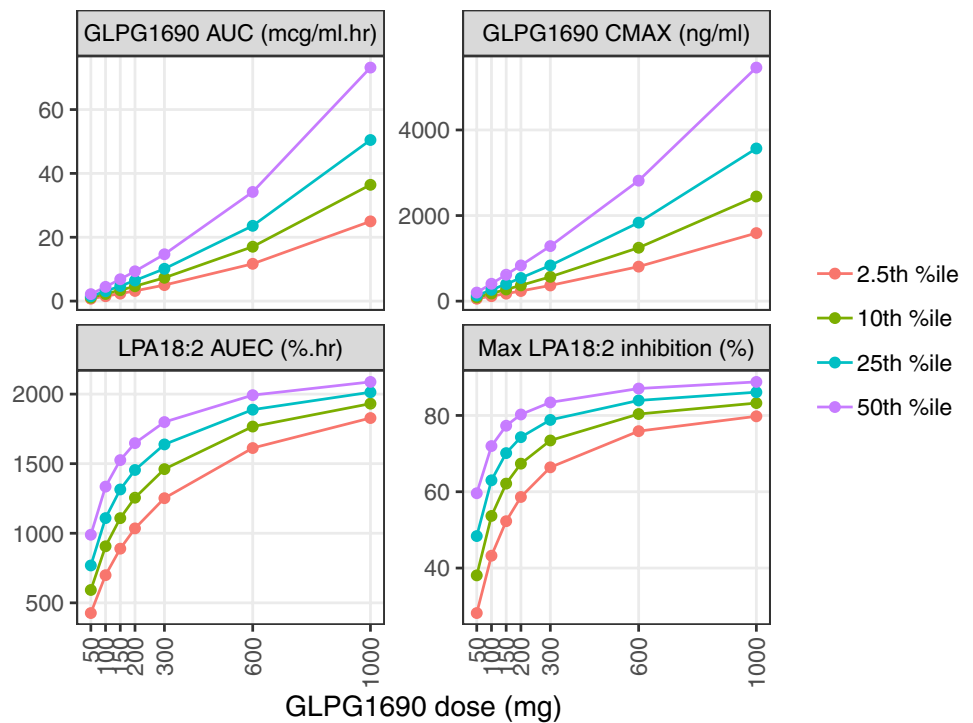
Fig. 8 Percentiles of individual-simulated fractions of the dosing interval where plasma concentrations of GLPG1690 lie above the 50% inhibitory concentration value (top), 80% inhibitory concentration value (middle), or 90% inhibitory concentration value (bottom) at doses between 50 and 1000 mg once daily. IC50/80/90 percentage of concentrations resulting in 50, 80, and 90% of the maximal effect

with IPF. Furthermore, both formulation and rifampin administration were found to be covariates on the rate of absorption. The absorption rate was 16% higher for the capsule compared with the suspension, and 117% higher in the presence of rifampin as compared with the absence of rifampin. Relative bioavailability in the presence of rifampin

was 10% of that in its absence. Finally, higher LPA $C18:2_{BL}$ resulted in lower IC_{50} and higher I_{max}. For an LPA $C18:2_{BL}$ of 0.36, the maximal reduction of LPA C18:2 was 91%. The estimated I_{max} tended to be higher following multiple (94%) as compared with single (81%) doses (see Table 3).

Figures 4 and 5 show the goodness-of-fit plots of the population and individual predictions for the PK and the PK/PD model, respectively. The predictions appeared to scatter randomly around the line of unity, indicating an unbiased model. The slope of the regression line (Fig. 4) indicated a slight regression to the mean, which is commonly observed in population PK and PK/PD models. In Fig. 4a, b, a small number of samples from the DDI study appeared above the scatter of dots, indicating a model over-prediction of these observations. Diagnostic plots (Fig. 4c–e) for both figures confirmed that the residuals were acceptable. Boxplots of population conditional weighted residuals (Figs. 4 and 5f) stratified by treatment group confirmed that the population PK and PK/PD model showed no meaningful bias with respect to dose and formulation.

Figure 6 shows VPCs of the full analysis dataset with good agreement between observed and simulated data for the majority of the analysis dataset. The simulated 95% CI of these statistics covered or almost covered the corresponding observed metrics on day 1 (left panel), with the model slightly over-predicting the dose-normalized GLPG1690 plasma concentration at the 97.5th percentile of the study population. The model slightly under-predicted the dose-normalized GLPG1690 plasma

Table 5 Summary of metrics of the individual patient simulations for treatment with GLPG1690 at steady-state doses between 200 and 600 mg once daily (QD)

Summary variable	200 mg GLPG1690 QD	300 mg GLPG1690 QD	600 mg GLPG1690 QD
Patients > IC_{50} for during the entire dosing interval (%)	24.7	43.4	79.8
Patients reaching 50% plasma LPA C18:2 reduction (%)	99.4	99.9	100
Patients reaching 80% plasma LPA C18:2 reduction (%)	51.3	69.7	91.0
Patients reaching 90% plasma LPA C18:2 reduction (%)	3.22	7.39	22.3
Median fraction of the dosing interval with GLPG1690 plasma concentration > IC_{50} (%)	79.0	94.0	100
Median fraction of the dosing interval with GLPG1690 plasma concentration > IC_{80} (%)	36.0	51.0	82.0
Median fraction of the dosing interval with GLPG1690 plasma concentration > IC_{90} (%)	0	20.0	54.0

IC_{50}, IC_{80}, IC_{90} 50%, 80%, 90% inhibitory concentration value, respectively, *LPA* lysophosphatidic acid
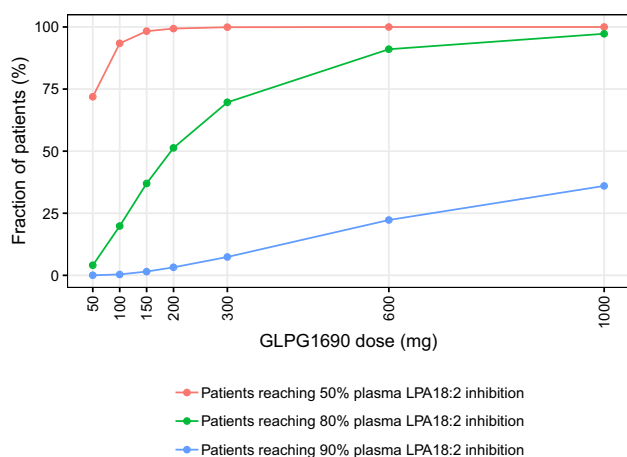
Fig. 9 Fraction of individual-simulated patients reaching 50, 80, and 90% reductions of plasma lysophosphatidic acid (LPA) C18:2 at GLPG1690 doses between 50 and 1000 mg once daily

concentration at the 2.5th percentile of the population during the 48 h after the dose on day 14 (right panel). While the average and variability of plasma LPA C18:2 was generally well described on both days 1 and 14, the plasma LPA C18:2 at 24 h after the dose on day 14 was lower than expected and not well described by the model.

3.4 Model-Based Simulations

Table 4 shows the simulated AUC_{24h}, $AUEC_{24h}$, C_{max}, and maximal plasma LPA C18:2 reduction (with 95% CI) at steady state for GLPG1690 across a range of dosing regimens between 50 mg QD and 1000 mg BID for the typical patient with IPF. The simulations showed that a dose of 200 mg QD led to an 81% (79–83%) LPA C18:2 reduction, and at a dose of 600 mg QD, the expected reduction was 88% (86–89%).

Figure 7 also shows visualizations of the 50th, 25th, 10th, and 2.5th percentiles of individual simulated GLPG1690

C_{max} and AUC, and a maximal plasma LPA C18:2 reduction and AUEC within the 50- to 1000-mg QD dose range. The impact of between-patient variability is illustrated by the difference between the curves representing different percentiles of the simulated population in each panel. There was an increasing response when raising the GLPG1690 dose from 200 to 300 and 600 mg QD for all summary variables. The curvature of the relationship between GLPG1690 dose and AUC reflects the implicit dose dependence on CL (estimated to decrease by approximately 4% per 100-mg increase of the GLPG1690 dose) included in the developed model (also see Fig. S3 of the ESM).

Most simulated patients reached a 50% reduction at 200 mg QD, with limited improvement in this metric when increasing the dose to 600 mg QD, indicating a high potency for LPA C18:2 reduction. Figure 8 summarizes the percentiles of individual-simulated fractions of the steady-state dosing interval above IC_{50} (114 ng/mL, see Table 5), IC_{80} (defined as 80%/20% times IC_{50}), and IC90 (90%/10% times IC_{50}) at GLPG1690 doses between 50 and 1000 mg QD. The first panel shows that 75% of the simulated patients have a GLPG1690 plasma concentration above the IC_{50} for the entire dosing interval at doses of at least 600 mg QD. In comparison, in 10% of patients treated with 600 mg QD, the GLPG1690 plasma concentration did not reach IC_{90}.

Figure 9 summarizes the percentiles of the fractions of simulated patients achieving 50, 80, or 90% reductions in LPA C18:2 as compared to baseline levels for a dose range from 50 to 1000 mg QD. Almost 75% of simulated patients reached the IC_{50} at the lowest simulated dose of 50 mg of GLPG1690 QD. At 150 mg, nearly all simulated patients (> 98%) reached IC_{50}. The higher targets of IC_{80} and IC_{90} showed a more pronounced dose–response relationship with the fraction of simulated patients reaching IC_{90} increasing from essentially none (< 0.1%) to 36% when increasing the GLPG1690 dose from 50 to 1000 mg QD. The fraction of patients reaching IC_{80} was the most sensitive of the three

summary metrics, increasing from 4% to 97% across the range of simulated GLPG1690 doses.

A summary of simulations for selected dosing regimens shows improved response with an increasing dose of GLPG1690 from 200 to 300 and 600 mg QD (Table 5). Almost all simulated patients reached a 50% reduction at 200 mg QD (99.4%) and an 80% reduction at the highest dose of 600 mg QD (91.0%).

4 Discussion

The pharmacokinetics of GLPG1690 was found to be adequately described by a two-compartment model with first-order absorption and dose-dependent elimination. Systemic clearance was found to decrease with increasing doses by approximately 4% for a 100-mg increase in GLPG1690 dose. Baseline covariates were included in the model to explain between-patient variability. Patient health status was identified as a significant and highly impactful covariate on the central volume of distribution, indicating an approximately 560% increase in volume in patients with IPF compared with HVs. This apparent disparity was most likely the result of a sparse sampling strategy in the PoC study, whereby PK samples were not taken around the time to C_{max}, resulting in an underestimation of the C_{max} [17]. Absorption rate was estimated to be 16% higher for GLPG1690 administered as an oral capsule compared with a suspension. However, the overall exposure was comparable between HV and patients with IPF who received the capsule formulation in the IPF patient study. Furthermore, absorption rate was 117% higher in the presence of rifampin compared to without rifampin. Co-administration with rifampin also affected the relative bioavailability, which was estimated at 10% compared to the bioavailability without rifampin without impacting the clearance of GLPG1690. Hence, rifampin co-administration did not impact the elimination of GLPG1690, but rather its absorption and bioavailability, resulting in decreased exposure [18]. Rifampin induces both intestinal P-gp as well as CYP3A4 [19]. As GLPG1690 has been shown to be a substrate of CYP3A4 and P-gp in an in vitro assay, we hypothesize that induction of the efflux transporter P-gp at the gut level was likely the explanation of the effect observed of rifampin on decreasing GLPG1690 exposure. To date, this hypothesis has not been confirmed by clinical data.

GLPG1690 caused an extensive and sustained reduction of LPA C18:2. A PK/PD model was developed to characterize the plasma LPA C18:2 biomarker response predicted by the GLPG1690 plasma concentration. Exploratory analyses indicated that the extent of hysteresis between the GLPG1690 plasma concentration and plasma LPA C18:2 was short lived, precluding the use of a turnover model [20]. Nevertheless, a model including an effect of delayed ("effect-site") concentration was found to improve the description of the observed plasma LPA C18:2 data, as evidenced by a reduction in the OFV function. The PK/PD relationship was described by an I_{max} model, where the predictor of response was the model-predicted effective concentration. A higher baseline LPA C18:2 predicted both higher potency and efficacy (lower IC_{50} and higher I_{max}, respectively). It has been reported that LPA levels are higher in female individuals and our observations in the PoC study are in line with this report [21] (see Fig. S4, Table S1 in the ESM). Median baseline LPA C18:2 levels were 0.47 and 0.36 in female and male individuals, respectively; LPA reductions were thus higher in female individuals. It should be noted that the dataset did not have equal representation of female and male subjects, hence no firm conclusions can be made on this covariate at this stage, but this hypothesis merits further evaluation.

The model predicted the exposure that would theoretically result in a half-maximal reduction of LPA C18:2 response (IC_{50}) at 114 ng/mL GLPG1690, which is in the same order of magnitude as the relative potency established in the ex vivo human plasma assay (IC_{50}: 131 nM and 242 nM, i.e., 77.1–142 ng/mL).

The PD response was simulated in a typical patient by predicting exposures for GLPG1690 and a reduction in LPA C18:2 based on the developed PK/PD model. To summarize, our work suggest that the therapeutic dose would range between 200 and 600 mg QD, with a maximal reduction of plasma LPA C18:2 at steady state of 81% in the typical patient following 200 mg QD, and practically all simulated patients reaching plasma concentrations above the IC_{50}. To avoid disrupting the physiological functions mediated by LPA C18:2, higher levels of reduction may be undesirable, and may be difficult to achieve because LPA production can occur along multiple pathways [1]. Similarly, the fraction of the dosing interval with concentrations above the IC_{50} was considerable at these doses, with half of the simulated patients predicted to maintain GLPG1690 plasma concentrations above the LPA C18:2 IC_{50} for at least 79% of the dosing interval at 200 mg QD.

The relationship between the clinical endpoint [absolute and relative forced vital capacity (FVC)], LPA C18:2, and GLPG1690 exposures was explored (data not shown); however, no correlations were evident. This could be attributed to the fact that there was only one active dose in the PoC study (600 mg QD), which precluded characterization of these putative relationships. However, the patients in the GLPG1690 arm showed a stabilization in their FVC measurements. Concurrently, statistically significant reductions in LPA C 18:2 vs. placebo were seen [13]. While a link between the LPA reduction and the clinical endpoint is yet to be established, the stabilization of the FVC observed in

the GLPG1690-treated arm in the POC study is in line with our predictions of the maximal inhibition of LPA occurring at a dose of 600 mg QD.

This was a limitation of the design of the current IPF patient study, and future trials would need to be conducted with multiple-dose cohorts to elucidate a relationship between the biomarker and the clinical endpoint. From a safety standpoint, GLPG1690 was found to be safe and well tolerated when administered to 17 patients with IPF at daily doses of 600 mg for a period of 12 weeks. The incidence of treatment-emergent adverse events was 64.7% in the placebo group and 66.7% in the GLPG1690 group [13]. GLPG1690 was also well tolerated in the multiple ascending dose study where it was administered at daily doses of 1000 mg daily for 14 days to a cohort of HVs. Overall, the treatment-emergent adverse events were of mild to moderate severity. Given the small sample sizes, these findings need to be confirmed in larger trials with more heterogeneous patient populations.

5 Conclusions

Based on these results, 200 and 600 mg QD doses were selected for future clinical trials in patients with IPF.

Compliance with Ethical Standards

Ethics Approval All procedures performed in studies involving human participants were in accordance with the ethical standards of the institutional and/or national research committee and with the 1964 Declaration of Helsinki and its later amendments or comparable ethical standards.

Consent to Participate Informed consent was obtained from all individual participants included in the clinical studies referred to in this article.

References

1. Tager A, LaCamera P, Shea B, Campanella G, Selman M, Zhao Z, et al. The lysophosphatidic acid receptor LPA1 links pulmonary fibrosis to lung injury by mediating fibroblast recruitment and vascular leak. Nat Med. 2008;14:45–54.
2. Gennero I, Laurencin-Dalicieux S, Conte-Auriol F, Briand-Mésange F, Laurencin D, Rue J, et al. Absence of the lysophosphatidic acid receptor LPA1 results in abnormal bone development and decreased bone mass. Bone. 2011;49:395–403.
3. Matas-Rico E, Garcia-Diaz B, Llebrez-Zayas P, López-Barroso D, Santin L, Pedraza C, et al. Deletion of lysophosphatidic acid receptor LPA1 reduces neurogenesis in the mouse dentate gyrus. Mol Cell Neurosci. 2008;39:342–55.
4. Ye X, Hama K, Contos J, Anliker B, Inoue A, Skinner M, et al. LPA3-mediated lysophosphatidic acid signalling in embryo implantation and spacing. Nature. 2005;435:104–8.
5. Sumida H, Noguchi K, Kihara Y, Abe M, Yanagida K, Hamano F, et al. LPA4 regulates blood and lymphatic vessel formation during mouse embryogenesis. Blood. 2010;116:5060–70.
6. Bandoh K, Aoki J, Taira A, Tsujimoto M, Arai H, Inoue K. Lysophosphatidic acid (LPA) receptors of the EDG family are differentially activated by LPA species: structure-activity relationship of cloned LPA receptors. FEBS Lett. 2000;478:59–65.
7. Scherer M, Schmitz G, Liebisch G. High-throughput analysis of sphingosine 1-phosphate, sphinganine 1-phosphate, and lysophosphatidic acid in plasma samples by liquid chromatography-tandem mass spectrometry. Clin Chem. 2009;55(6):1218–22. https://doi.org/10.1373/clinchem.2008.113779.
8. Georas S, Berdyshev E, Hubbard W, Gorshkova I, Usatyuk P, Saatian B, et al. Lysophosphatidic acid is detectable in human bronchoalveolar lavage fluids at baseline and increased after segmental allergen challenge. Clin Exp Allergy. 2007;37:311–22.
9. Park G, Lee Y, Berdyshev E, Nyenhuis S, Du J, Fu P, et al. Autotaxin production of lysophosphatidic acid mediates allergic asthmatic inflammation. Am J Respir Crit Care Med. 2013;188:928–40.
10. Desroy N, Housseman C, Bock X, Joncour A, Bienvenu N, Cherel L, et al. Discovery of 2-[[2-ethyl-6-[4-[2-(3-hydroxyazetidin-1-yl)-2-oxoethyl]piperazin-1-yl]-8-methylimidazo[1,2-a]pyridin-3-yl]methylamino]-4-(4-fluorophenyl)thiazole-5-carbonitrile (GLPG1690), a first-in-class autotaxin inhibitor undergoing clinical evaluation for the treatment of idiopathic pulmonary fibrosis. J Med Chem. 2017;60(9):3580–90.
11. Ongenaert M, Dupont S, Blanqué R, Brys R, van der Aar E, Heckmann B. Strong reversal of the lung fibrosis disease signature by autotaxin inhibitor GLPG 1690 in a mouse model for IPF. European Respiratory Society London, 2016. Available from: http://www.glpg.com/docs/view/57d15f03ac163-en. Accessed 25 Jan 2019
12. Van der Aar EM, Fagard L, Desrivot J, Dupont S, Heckmann B, Blanque R, Gheyle L, Ralic J, Vanhoutte F. Favorable human safety, pharmacokinetics, and pharmacodynamics of the autotaxin inhibitor GLP1690, a potential new treatment in IPF. In: Poster presented at the American Thoracic Society Conference; 2016 May 13–18; San Francisco (CA).
13. Maher TM, van der Aar EM, Van de Steen O, Allamassey L, Desrivot J, Dupont S, et al. Safety, tolerability, pharmacokinetics,

and pharmacodynamics of GLPG1690, a novel autotaxin inhibitor, to treat idiopathic pulmonary fibrosis (FLORA): a phase 2a randomised placebo-controlled trial. Lancet Respir Med. 2018;6(8):627–35.

14. Fieuw A, Van der Aar EM, Fagard L, Stutvoet S, Desrivot J, Dupont S, Allamassey L, Van de Steen O. GLPG1690, a potential new treatment in idiopathic pulmonary fibrosis: design of the first-in-patient clinical study. In: Poster presented at the Pulmonary Fibrosis Foundation Summit; 2017 Nov 9–11; Nashville (TN).

15. US Food and Drug Administration. Guidance for industry: population pharmacokinetics. Rockville (MD): US Food and Drug Administration. 1999. http://www.fda.gov/downloads/Drugs/GuidanceComplianceRegulatoryInformation/Guidances/ucm072137.pdf.[Accessed 13 Mar 2019.

16. European Medicines Agency. Guideline on reporting the results of population pharmacokinetic analyses. London: European Medicines Agency. 2007. http://www.ema.europa.eu/docs/en_GB/document_library/Scientific_guideline/2009/09/WC500003067.pdf. Accessed 13 Mar 2019.

17. Mehvar R. The relationship among pharmacokinetic parameters: effects of altered kinetics on the drug plasma concentration-time profiles. Am J Pharm Educ. 2004;68(2):1–9.

18. Chen J, Raymond K. Roles of rifampicin in drug-drug interactions: underlying molecular mechanisms involving the nuclear pregnane X receptor. Ann Clin Microbiol Antimicrob. 2006;15(5):3.

19. Hanke N, Frechen S, Moj D, Britz H, Eissing T, Wendl T, et al. PBPK models for CYP3A4 and P-gp DDI prediction: a modeling network of rifampicin, itraconazole, clarithromycin, midazolam, alfentanil, and digoxin. CPT Pharmacomet Syst Pharmacol. 2018;7(10):647–59.

20. Dayneka NL, Garg V, Jusko WJ. Comparison of four basic models of indirect pharmacodynamic responses. J Pharmacokinet Biopharm. 1993;21(4):457–78.

21. Michalczyk A, Budkowska M, Dołęgowska B, Chlubek D, Safranow K. Lysophosphatidic acid plasma concentrations in healthy subjects: circadian rhythm and associations with demographic, anthropometric and biochemical parameters. Lipids Health Dis. 2017;16(1):140.